



Cite this: *RSC Pharm.*, 2026, **3**, 247

Alditols in complex with boronophenylalanine for improving aqueous solubility for boron neutron capture therapy

Teng-San Hsieh,^a Yu-Hou Yu,^b Zhen-Fan You,^b Rong-Jiun Sheu,^c Jin-Pei Deng^d and Chung-Shan Yu ^{a,c}

Boron neutron capture therapy (BNCT) aimed at treating brain tumors is deteriorated by the poor aqueous solubility of the BNCT agent, boronophenylalanine (BPA). Solubilizers, such as sorbitol, mannitol and xylitol and their mixing formulas, the storage temperature and time, acid adjusters, and antioxidants, as well as lyophilization conditions were studied. HPLC, ¹H-NMR, and scanning electron microscopy (SEM) were used to investigate the alditol–BPA samples. HPLC results showed that the stability of sorbitol–BPA samples improved when the antioxidant Na₂S₂O₅ was used, 98.25 ± 0.31% vs. 94.37 ± 1.24%, *P* < 0.05. The osmolality ratio of sorbitol–BPA, 0.83 ± 0.03, was lower than that of saline, 1.0, making it physiologically compatible. SEM results of the lyophilized samples showed a proportion of sorbitol–BPA vs. H₂O in a molar ratio of 1:10. Sorbitol was the best solubilizer according to the ¹H-NMR-derived integral ratio in the decreasing order of sorbitol–BPA, mannitol–BPA, fructose–BPA and xylitol–BPA with the values of 12.15 ± 1.30, 6.65 ± 0.61, 6.13 ± 1.90 and 4.77 ± 0.72, *P* < 0.05, respectively. The antioxidant Na₂S₂O₅ improved the stability of sorbitol–BPA at 25 °C according to the ¹H-integral ratio of 17.60 ± 2.15 vs. 12.67 ± 1.62, *P* = 0.10. The differences were not statistically significant. From both the HPLC and ¹H-integral results, sorbitol emerges as the optimal solubilizer for BPA for further *in vivo* studies.

Received 9th July 2025,
Accepted 14th November 2025
DOI: 10.1039/d5pm00180c
rsc.li/RSCPharma

1. Introduction

Boron neutron capture therapy (BNCT) is a binary technology for treatment of tumors, mostly for recurrent brain tumors.^{1,2} The enriched ¹⁰B atom is covalently bonded to bioactive molecules. Once they accumulate in the tumor lesion, the subsequent bombardment of the epithermal neutrons from an external beam source can produce fused unstable ¹⁰B particle composites. Such a composite can split into two particles with linear energy transfer. The two highly energetic particles of ⁷Li and the alpha ion (⁴He⁺) can damage the surrounding tumor cells within a cell-diameter range.^{1,3–7}

BNCT agents require (1) low intrinsic toxicity, (2) high tumor uptake (~20–50 µg ¹⁰B), (3) selective uptake in tumors with a ratio greater than 3 and (4) relatively rapid clearance from blood and normal tissues.² Boron clusters or boron cages, such as

BSH and nanoparticles, are used to coordinate boron atoms for delivery.^{8–10} These conjugates are advantageous because of their higher loading of ¹⁰B atoms. Significant damage to the tumor cells would be possible if they can be targeted to the tumor cells. Evaluation of the delivery efficiency *in vivo* is important for modifying the molecular targeting.^{11,12} When examining the tumor types on a clinical basis, brain tumors might be an obstacle for these big particles to freely transport across the blood–brain barrier.¹³ Such a barrier is also a big obstacle for small molecules. Only very few of them can be developed as pharmaceuticals for brain tumor therapy.

Among the BNCT agents studied so far, boronophenylalanine (BPA) is the most advanced in the preclinical stage (Fig. 1).^{2,14–16}

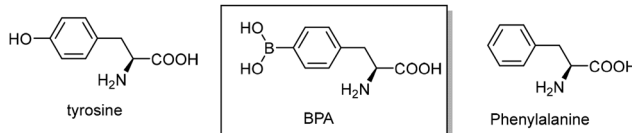


Fig. 1 Two potential degraded metabolites, tyrosine and phenylalanine, are used as authentic standards to analyze the HPLC chromatograms of the lyophilized alditol–BPA samples stored over various timelines.

^aDepartment of Biomedical Engineering and Environmental Sciences, National Tsinghua University, Hsinchu 30013, Taiwan. E-mail: csyu@mx.nthu.edu.tw

^bHerong Neutron Medical Corporation, Hsinchu 30261, Taiwan

^cInstitute of Nuclear Engineering and Science, National Tsinghua University, Hsinchu, 30013, Taiwan

^dDepartment of Chemistry, Tamkang University, Tamsui, New Taipei City 251301, Taiwan



Serving as one of the essential amino acid nutrients for brain metabolism, phenylalanine is an ideal vehicle for delivering boron-10 atoms for targeting BNCT. Being structurally similar to phenylalanine, BPA may cross the BBB through the LAT-1 transporter, a membrane protein abundantly over-expressed in brain tumors.¹⁴ However, due to its poor aqueous solubility (1.6 g L^{-1}), a sufficient amount of ^{10}B atoms (900 mg kg^{-1}) is barely achieved during clinical treatment of a patient. Hence, fructose is used as a complexing agent with the diol groups of BPA through dehydration to attain the above concentration requirement (Fig. 2 and 3). The limited shelf life of fructose–BPA is a drawback. For example, the solution formulation can last for 12 days in storage in the dark at room temperature or $2\text{--}8^\circ\text{C}$.^{17,18} Moreover, its equilibrated open keto or aldehyde form is readily attacked by amino groups of other proteins *in vivo*. This may alter its physiological function and result in unexpected biological side effects, *e.g.* lactic acidosis and even fatalities.

Hence, without forming anomers, the alditols produced from reduced aldoses would be an alternative candidate (Fig. 2).

For the purpose of applying the formulation of BPA in humans, a pH value of 7.4 is required to meet physiological conditions. Inorganic acids such as HCl are mostly used to adjust the alkalinity when preparing the sample of fructose–BPA. Organic acids, such as gluconic acid and sialic acid, with both carboxylic acid and polyhydroxy groups, exert both complexation and pH adjustment. These dual functionalities may reduce the amount of reagent required for solubilization, thereby reducing the osmolality.

2. Materials and methods

2.1 General

A Vortex Genie 2 was used for the 60 mg-scale preparation. A laboratory magnetic stirrer at 1000 rpm or higher was used for one-gram and 3-gram scale preparations. All alditols, BPA, reagents and HPLC solvents were purchased from Acros (Geel, Belgium) and Alfa (Binfield, Berkshire, UK). NMR spectroscopy, including ^1H -NMR (500 MHz), was performed on a Bruker Avance 500 MHz instrument (Bruker, Germany). The deuterated-solvent D_2O employed for NMR spectroscopy was purchased from Aldrich (St. Louis, MO, USA). The HPLC system comprised an Agilent 1100 series quaternary pump G1311A, which is coupled with a column Chempack Chemcisorb 7-ODS-H 5 μm $10 \times 250 \text{ mm}$ and equipped with a stand of the G1328B manual injector and Rheodyne injector 7725i with a 500 μL loop. The sample was eluted through a UV detector G1314A with a flow cell G1314-60086 4 MPa at 260 nm using isocratic eluents: 80% CH_3OH (aq.) at a flow rate of 3 mL min^{-1} .

Osmotic pressure measurement was performed using Advanced Instruments, Model 3320 Osmometer at Institute of Biological Medicine, Industrial Technology Research Institute, Taiwan. Scanning electron microscopy was performed using a High Resolution Thermal Field Emission Scanning Electron Microscope JEOL, JSM-7610F at National Tsinghua University. Graphpad prism V was used to generate the statistical data. Student's *t*-test and analysis of variance (ANOVA) models were used for two and more than two groups of data and the *P*-value of 0.05 was set as the standard. *P* values were provided in some cases when larger standard deviation was obtained.

2.2 BPA–saccharide complex preparation

2.2.1 60 mg-scale preparation. To an Eppendorf tube (5 mL) was added an aliquot of 2 mL of 0.15 N NaOH (aq.) and BPA (60 mg), sequentially. The mixture was vigorously vibrated at full-scale power for 2 min using a vortex shaker. After adding 64 mg of alditols, the full-scale vibration was continued for 10–15 min. The solution concentration was controlled at 3.0% W/V for BPA and at 3.2% W/V for alditols. The mixture with an initial pH of 8.5 was first adjusted to 8.0 by adding 6 N HCl (1–8 μL) and subsequently through additional 3 N HCl ($\sim 15 \mu\text{L}$) to the desired pH values 7.6, 7.4, 7.2 and 7.0, respectively. After filtration using a 0.22 μm membrane filter, the filtrate was transferred to another Eppendorf tube (5 mL) for subsequent immersion in a Dewar flask containing liquid N_2 for 5 min. The frozen sample was lyophilized under 0.1 Pa at 20°C for 18 h and at 25°C for 6 h (Fig. 4). The yield was 75%. The workflow can be found in the SI.

2.2.2 One-gram protocol. To a wide-neck PP bottle (50 mL) were added NaOH (0.15 N, 40 mL), BPA (1.2 g) and the alditols (1.28 g), sequentially. Stirring was performed with a magnetic stirrer in a full power mode using 1000 rpm or more. The acid portions of 6 N HCl (75 μL) and 3 N HCl (20 μL) were used, respectively. The filtration was performed with a PTFE membrane filter, 0.20 μm with 47 mm ID. The filtrates were distributed over 4 PP bottles (50 mL) and the subsequent lyophilization

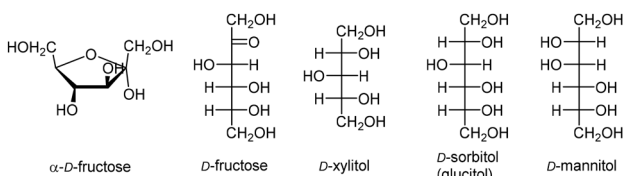


Fig. 2 Saccharide and its reduced forms used for this complexation and the dissolution study.

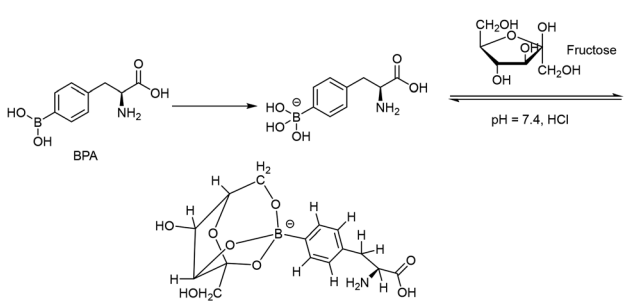


Fig. 3 Reported formation of the fructose–BPA complex for improving aqueous solubility.^{19,20}



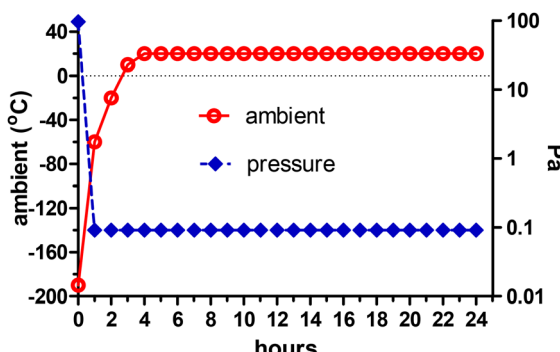


Fig. 4 Lyophilization conditions employed for the formation of alditol-BPA complexes.

was performed as described above. The setup can be found in the SI. A white soft solid was obtained in 82.8% yield (2.05 g).

2.2.3 3-Gram scale protocol. To a 250 mL wide-neck pp bottle were added NaOH (aq., 0.15 N, 100 mL), BPA reagent (3 g) and the alditols (3.2 g), sequentially. Stirring was also performed with a magnetic stirrer at a full power mode with at least 1000 rpm. The acid portion of 6 N HCl (245 μ L) was used straightforwardly to attain pH = 7.4. Filtration was performed with a PTFE membrane filter, 0.20 μ m with 47 mm ID. The filtrates were distributed over 10 PP bottles (50 mL). The lyophilization procedure was the same as above, and a white solid was obtained in 82.2% yield (5.1 g).

2.2.4 Dual formula preparation. The preparation is the same as that performed for 2.2.1. To an Eppendorf tube (5 mL) were added an aliquot of 2 mL of 0.15 N NaOH (aq.) and BPA (60 mg), sequentially. The mixture was vigorously vibrated using full-scale power for 2 min using a vortex shaker. After adding 64 mg of alditols in the desired mixing ratio, the full-scale vibration was continued for 10–15 min. The subsequent procedure followed that of section 2.2.1.

2.3 Auxiliary formulation

The procedure was the same as that used for 60 mg-scale preparation. A stock solution of sialic acid was prepared from 1 g sialic acid (SA) in H_2O (5 mL). The acidity was approximated to be about 2 M comparable to 3 N HCl. Commercial gluconic acid (GA) obtained as a solution in 6.4 M was directly used. After the alkaline mixture turned clear, an inorganic acid solution of 6 N HCl was added first to the mixture to reach pH 8.0. SA or GA were added until the desired pH values of 7.6, 7.4, 7.2 and 7.0 were obtained (\sim 30 μ L).

In the preparation using an antioxidant, $\text{Na}_2\text{S}_2\text{O}_5$ was prepared in a concentration of 5 g per 100 mL (aq.) and 4 μ L was added to the solution whose pH has been adjusted. In the case of ascorbic acid, the same concentration of 5 g per 100 mL and the same volume (4 μ L) were used.

2.4 High-performance liquid chromatography (HPLC) preparation

The suspected degraded byproducts, tyrosine and phenylalanine, were confirmed in each chromatography. These auth-

entic samples were prepared in 5 mg per 0.5 mL. Two aliquots (5 and 10 μ L) were intentionally mixed with the alditol-BPA samples for injection, respectively. The identities of the unknown peaks from alditol-BPA could be confirmed. The same method was also applied to the other potentially degraded byproduct, tyrosine. Alditol-BPA samples may show broadened peaks due to tailoring in the case of xylitol-BPA. Such a sample might be due to the hardened appearance after storage. We also noted a pH increase from 0.2 to 0.4 after dissolution. HPLC results of a two-component formula such as SA/sorb-BPA showed asymmetric peak patterns. This did not seriously disturb the identification of the byproducts. The baselines of the chromatograms all appeared reasonably.

3. Results and discussion

We studied the factors that may affect the preparation, the dissolution, and the physical and chemical properties of BPA samples. Solubilizers such as three alditols and their mixing formulas, the storage temperature and time, acid adjusters and antioxidants as well as lyophilization protocols are the issues to be studied.

The physical appearance of the lyophilized samples after storage and dissolution was also compared with the chromatographic and spectroscopic data from HPLC and $^1\text{H-NMR}$. In addition, scanning electron microscopy (SEM) was also used to investigate the network of the lyophilized samples.

Improving the solubility of BPA using alditols such as mannitol and sorbitol has been reported.^{18,21} The side effects were also noted. For example, mannitol was associated with diuresis. Its 2-epimer, sorbitol, with relatively high osmotic pressure may limit the loading of more boron atoms.^{21,22} Therefore, osmotic pressure of our samples was measured to evaluate their physical compatibility.

During lyophilization, the conventional precooling conditions at $-78\text{ }^\circ\text{C}$ through indirect gas–liquid contact were time-consuming.²³ The straightforward immersion into liquid N_2 solution *via* liquid–liquid direct contact can shorten the precooling time. Subsequent lyophilization was performed under 0.1 Pa at 20 $^\circ\text{C}$ for 18 h and 25 $^\circ\text{C}$ for 6 h (Fig. 4). The present laboratory-scale lyophilization makes the procedure facile.

3.1 Physical chemical description of the samples after lyophilization, storage and dissolution

In general, the lyophilized samples after storage for more than 3 months could be dissolved in H_2O within 1 min. Some examples such as the room-temperature-stored xylitol-BPA samples with a solidified appearance were difficult to break. They required a longer dissolution time, *ca.* 1–3 min, compared with sorbitol-BPA in less than 15 s. The solution state could last for 2 days without precipitation. These lyophilized samples were found to degrade into two byproducts *i.e.* tyrosine and phenylalanine (Fig. 1). HPLC was used to analyze these degraded byproducts. The HPLC chromatograms indi-

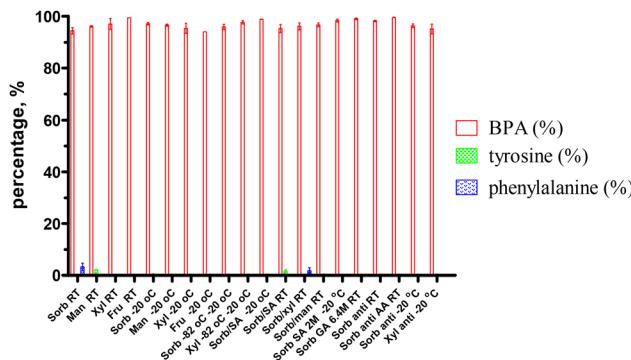


Fig. 5 Stability analysis of the BPA–alditol mixture through HPLC. The intact BPA and degraded byproducts tyrosine and phenylamine are shown. Antioxidation: $\text{Na}_2\text{S}_2\text{O}_5$, RT: room-temperature storage, $-20\text{ }^\circ\text{C}$: $-20\text{ }^\circ\text{C}$ storage, $-82\text{ }^\circ\text{C}$: freezing was performed at $-196\text{ }^\circ\text{C}$ unless specified, $^{\$}$ Sorb: sorbitol, SA: sialic acid, Xyl: xylitol, Man: mannitol, Fru: fructose, GA: gluconic acid, AA: ascorbic acid as the antioxidant, dual formula: sorbitol + sialic acid ranging from 2:1 to 7:1, sorbitol + xylitol ranging from 1:2 to 3:1 and sorbitol + mannitol ranging from 2:3 to 4:1.

cated their gradual increase, as shown in Fig. 5 and SI, Table S12.

The boron content of the lyophilized samples was further analyzed by inductive coupled plasma mass analysis (ICP-MS). The boron was preserved in 80–90% compared to the samples prior to the preparation (data not shown). The loss of boron might be due to the filtration procedure for sterilization before lyophilization.

3.2 HPLC analyses

The HPLC data showed that sorbitol–BPA samples stored at $-20\text{ }^\circ\text{C}$ might be better than those stored at $25\text{ }^\circ\text{C}$, $97.17 \pm 0.48\%$ vs. $94.37 \pm 1.24\%$, $P = 0.18$ (Fig. 6). These differences are not statistically significant. The antioxidant $\text{Na}_2\text{S}_2\text{O}_5$ did improve the stability of the sorbitol–BPA group at $25\text{ }^\circ\text{C}$ from $98.25 \pm 0.31\%$ vs. $94.37 \pm 1.24\%$, $P < 0.05$ (Fig. 7).

When both the antioxidant and lower storing temperature of $-20\text{ }^\circ\text{C}$ were employed, the intact form in $96.36 \pm 0.72\%$ was

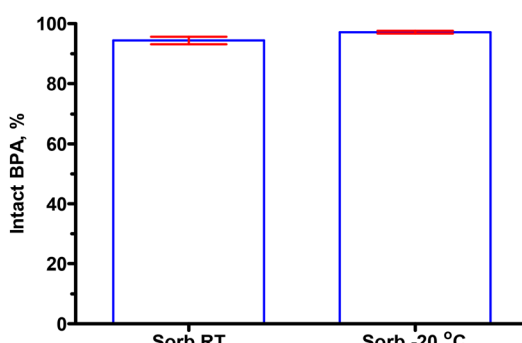


Fig. 6 HPLC results of the sorbitol–BPA samples. Comparison of the intact BPA samples after storage at $-20\text{ }^\circ\text{C}$ for 250 days and at $25\text{ }^\circ\text{C}$ for 221 days, $97.17 \pm 0.48\%$ vs. $94.37 \pm 1.24\%$, $P = 0.18$.

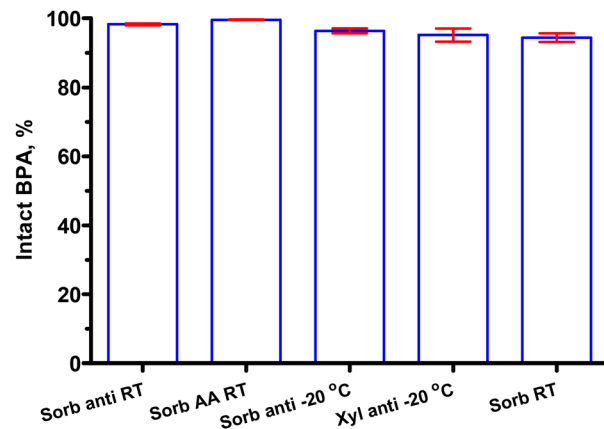


Fig. 7 HPLC results of the alditol–BPA samples. Comparison of the intact BPA% by examining the antioxidation effect, 98.25 ± 0.31 , 99.56 ± 0.11 , $96.36 \pm 0.72\%$, $95.14 \pm 1.92\%$, 94.37 ± 1.24 , $P < 0.05$ (from left). anti: $\text{Na}_2\text{S}_2\text{O}_5$ as the antioxidant, AA: ascorbic acid as the antioxidant.

not better than that at $25\text{ }^\circ\text{C}$, $98.25 \pm 0.31\%$, $P < 0.05$. Synergistic effects were not obtained. Although ascorbic acid (AA) was better than $\text{Na}_2\text{S}_2\text{O}_5$ from $99.56 \pm 0.11\%$ vs. $98.25 \pm 0.31\%$, $P < 0.05$, the relatively short storage of 47–81 days vs. 224 days may not be sufficient to judge the results. Similar results will be discussed in the section of ^1H -NMR study.

Acid adjusters using sialic acid might be better than the inorganic acid HCl, $98.38 \pm 0.53\%$ vs. $97.17 \pm 0.48\%$, $P = 0.15$ (Fig. 8). However, these differences are not statistically significant. 6.4 M gluconic acid was better than sialic acid according to $99.02 \pm 0.31\%$ vs. $98.38 \pm 0.53\%$, $P = 0.36$.

All these samples exhibited significant stabilities with less than 5% degraded byproducts after storage for 90–180 days. In addition, after a longer storage for more than 270 days, sorbitol–BPA preserved more intact fraction, 94–97%.

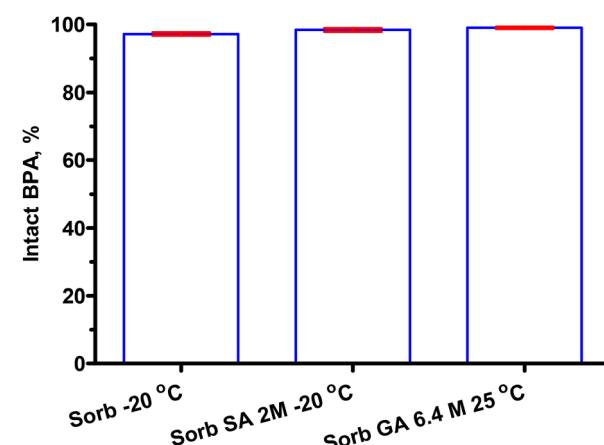


Fig. 8 HPLC results of sorbitol–BPA samples. Intact BPA% remained after using organic acid adjusters. $97.17 \pm 0.48\%$, $98.38 \pm 0.53\%$, $99.02 \pm 0.31\%$, $P = 0.06$ (from left).



3.3 Osmotic pressure analysis

Osmolality measurement results are shown in Fig. 9 and SI, Table S13. In general, the solution of these samples exerted a lower osmotic pressure ratio than that of saline, 0.49–0.99 vs. 1.0. Even in the group of double concentrated samples, the osmotic pressure ratio of 1.7–1.8 was still less than the expected ratio of 2.0 (data not shown). Notably, the xylitol-BPA group exhibited larger osmolality when compared with sorbitol-BPA and mannitol-BPA at $-20\text{ }^{\circ}\text{C}$ storage, 0.97 ± 0.11 vs. 0.83 ± 0.03 vs. 0.82 ± 0.03 , $P = 0.24$. However, these differences are not statistically significant. The finding was consistent with the inferior solubility of xylitol-BPA when dissolving the rock-like samples after storage for more than one month. The overall smaller osmolality ratio of 0.50–0.99 indicates the practicality of using the present protocol.

3.4 Morphological description

Field-emission scanning electron microscopy (SEM) was performed on a JEOL JSM-7610F at an acceleration voltage of 15.0 kV at magnifications ranging from 200 to 2500 fold. As displayed in Fig. 10a–j and a zoom-in image in Fig. 11, numerous holes were distributed over plastic-like plates. Notably, an irregular layer was also observed. These holes are suggested to be the water molecules evacuated after freeze-drying.

3.5 $^1\text{H-NMR}$ study

All the lyophilized samples were prepared in D_2O for subsequent $^1\text{H-NMR}$ experiment (Fig. 12).

Pure BPA samples were not soluble in D_2O and only precipitates were observed. Two larger peaks at 7.15 and 7.45 ppm are different from those of the free form, 7.25 and 7.65 ppm. The downfield is suggested to be the electron donating effect through the three *erythro* alkoxy groups and the anionic boron atom. The conjugated complex disrupts the BPA–BPA hydrogen bonding, thereby inducing a new hydrogen bond between the

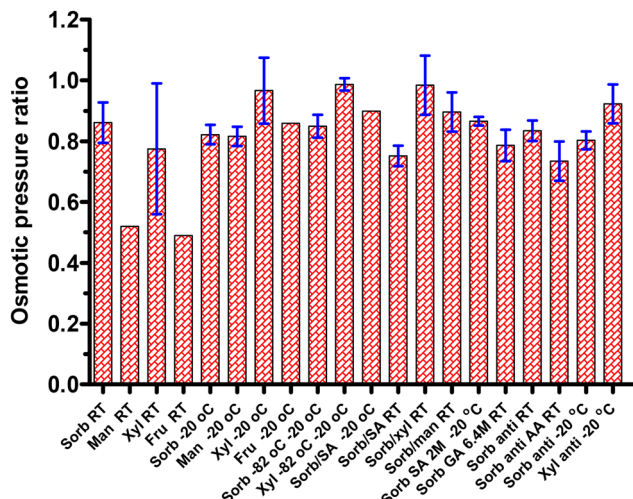


Fig. 9 Bar chart of the osmotic pressure ratios of the BPA–saccharide lyophilized samples after dissolution.

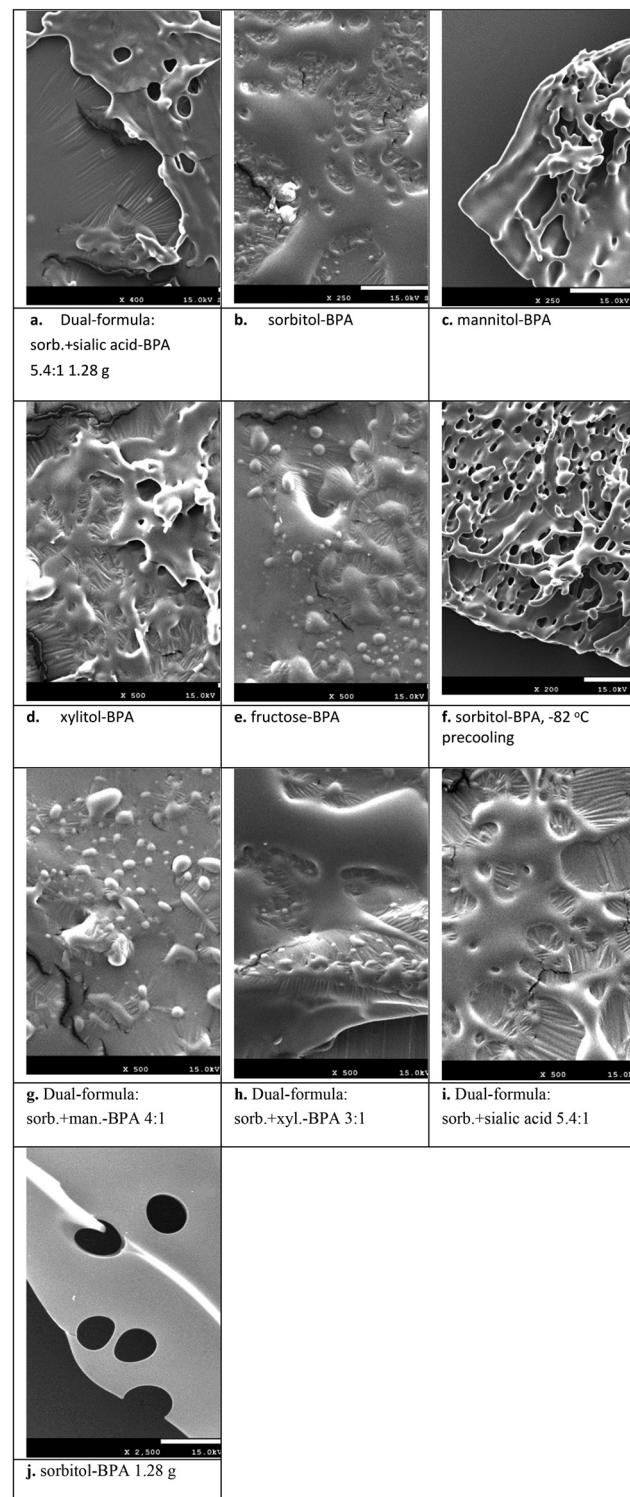


Fig. 10 The micrographs of the lyophilized alditol–BPA samples were obtained through scanning electron microscopy (SEM). Various zoom-in graphs were produced at a 200–2500 fold magnification. Samples obtained from conditions such as semipreparation (a and j), precooling at $-82\text{ }^{\circ}\text{C}$ (f) and dual-component formula (a, g–i) were employed. Numerous holes distributed over these plastic-like plates are suggested to be the space occupied by water molecules when evacuated after lyophilization.



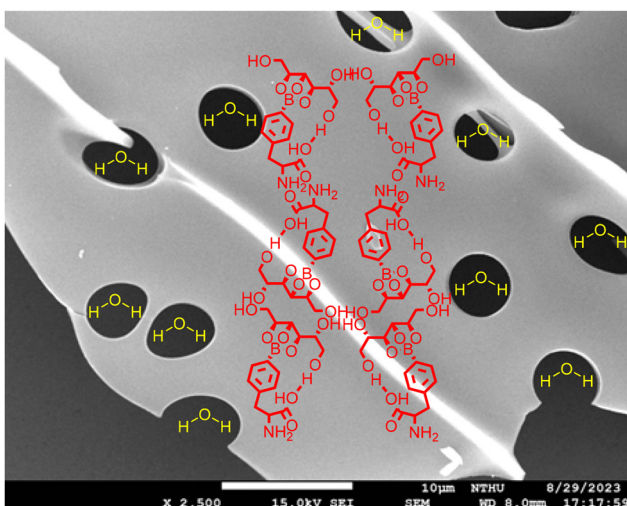


Fig. 11 The microstructures of Fig. 10j are envisaged as the polymerized plate formed by larger BPA–sorbitol molecular chains accompanied by the holes of water evacuated. A molar ratio of 10 for H_2O vs. BPA–sorbitol was assumed.

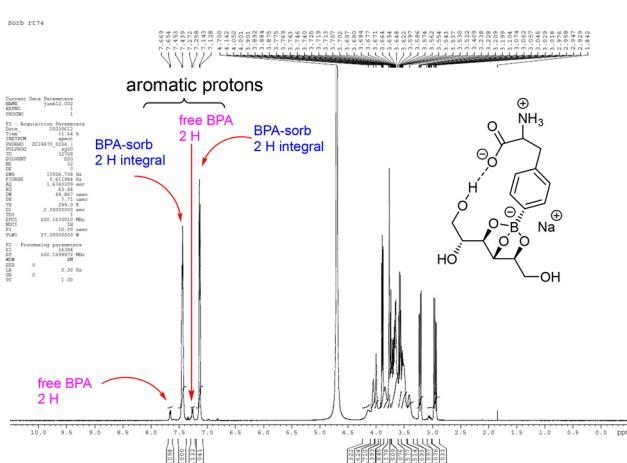


Fig. 12 Different chemical shifts of sorbitol–BPA from that of free BPA in aromatic regions are specified

complex of sorbitol-BPA and H₂O. Therefore, the ratio of aromatic ¹H-integrals of sorbitol-BPA *vs.* BPA can be regarded as an index of the aqueous solubility. The ¹H-integral ratio of the complexing conjugate alditol-BPA *vs.* free BPA is summarized in Fig. 13 and SI, Table S14.

Data of sorbitol-BPA, mannitol-BPA, xylitol-BPA and fructose-BPA from 25 °C and -20 °C storage were averaged to afford the integral ratios of $12.15 \pm 1.30\%$, $6.65 \pm 0.61\%$, $4.77 \pm 0.72\%$ and $6.13 \pm 1.90\%$, $P < 0.05$, respectively (Fig. 14). The highest ratio of sorbitol-BPA is also in agreement with the dissolution finding. The solution state of sorbitol-BPA remains the longest

The antioxidant $\text{Na}_2\text{S}_2\text{O}_5$ improved the stability of sorbitol–BPA at 25°C , 17.60 ± 2.15 vs. 12.67 ± 1.62 , $P = 0.10$ (Fig. 15). But the antioxidation effect was not significant at -20°C , 10.67 ± 2.12 vs. 11.37 ± 2.39 , $P = 0.84$. Similar to the former

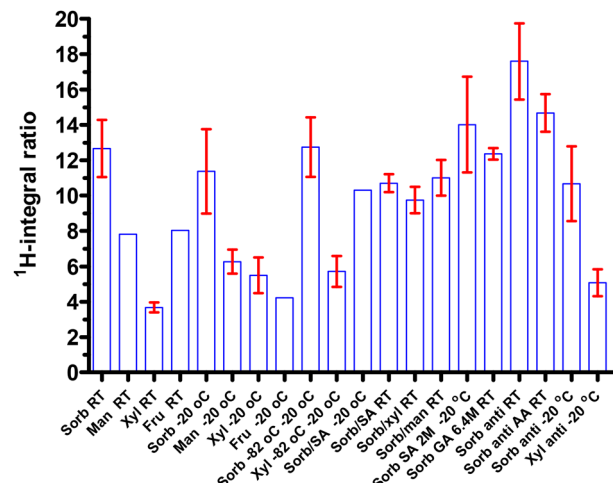


Fig. 13 The overall comparison of the ^1H -integral ratio of the alditol–BPA samples from this study. Bar chart of these ^1H -integral ratios for alditol–BPA samples was prepared under various conditions.

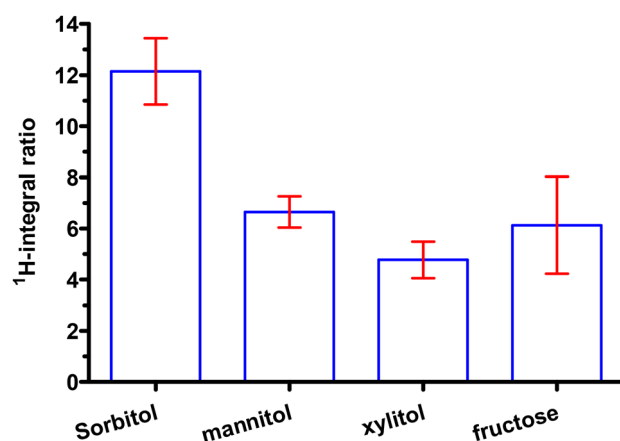


Fig. 14 Complexation ratios were affected through solubilizers. The ^1H -integral ratio of solubilizer–BPA to free BPA from $-20\text{ }^\circ\text{C}$ and $25\text{ }^\circ\text{C}$ -stored samples, 12.15 ± 1.30 , 6.65 ± 0.61 , 4.77 ± 0.72 and 6.13 ± 1.90 , $P < 0.05$ (from left).

HPLC results, the synergistic effect was not obtained. Ascorbic acid (AA) also benefited the complex formation, 14.68 ± 1.07 vs. 12.67 ± 1.62 , $P = 0.53$. The differences from the three examples are not statistically significant.

As shown in Fig. 16, the two organic acid adjusters *i.e.* sialic acid (SA) and gluconic acid (GA) both can improve the complexing ratio of BPA–sorbitol, 14.01 ± 2.71 *vs.* 12.36 ± 0.33 *vs.* 11.37 ± 2.39 , $P = 0.70$. However, these differences are not statistically significant. The dual-component formula did not improve the complexation ratio (Fig. 17).

From these comparisons, sorbitol exerts the best complexation with BPA.

As shown in Fig. 18a, sorbitol complexed with BPA in a stable conformation. Not only the *threo* OH groups were involved in forming the tetrahedral borate, but also the flexible backbone allowed an additional hydrogen bonding between

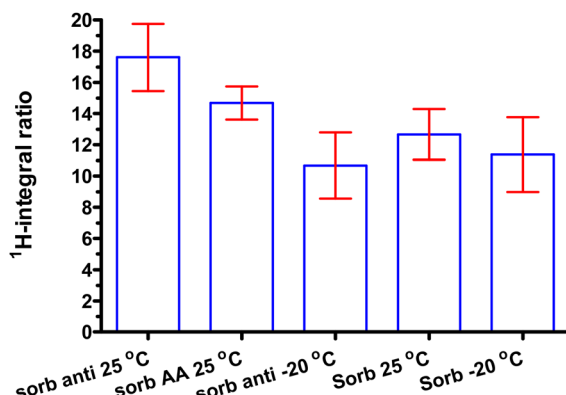


Fig. 15 The effects of antioxidants, $\text{Na}_2\text{S}_2\text{O}_5$ (anti) and ascorbic acid (AA), on the complexation ratio of sorbitol–BPA are compared, 17.60 ± 2.15 , 14.68 ± 1.07 , 10.67 ± 2.12 , 12.67 ± 1.62 , 11.37 ± 2.39 , $P = 0.20$ (from left).

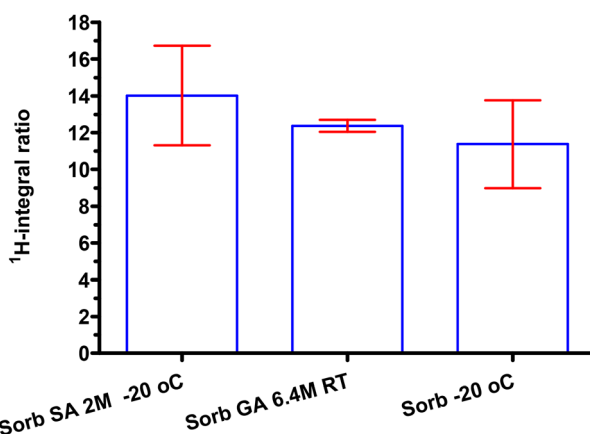


Fig. 16 Acid adjusters, sialic acid and gluconic acid affect the sorbitol–BPA complexing ratio, 14.01 ± 2.71 , 12.36 ± 0.33 , 11.37 ± 2.39 , $P = 0.70$ (from left).

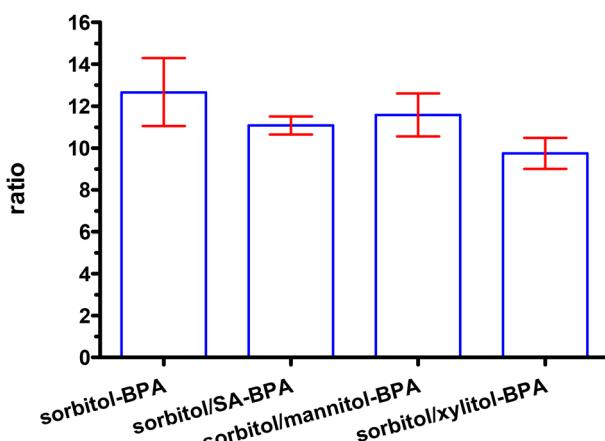


Fig. 17 Comparison of ^1H -integral in the dual-component formula in the complexation study, 12.67 ± 1.62 , 11.08 ± 0.43 , 11.59 ± 1.03 , 9.75 ± 0.75 , $P = 0.24$ (from left).

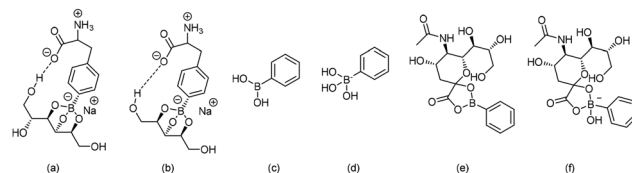


Fig. 18 Simulated sketch of the both (a) sorbitol–BPA and (b) xylitol–BPA showed energy minimization via extra hydrogen bond formation in addition to the covalent tetraborate formation through dehydration. The estimated complexation is obtained from software Chemdraw MM2 mode. Literature work shows the complexing modes of (c) phenyl boric acid (PBA) and (d) phenyl borate (PB) with sialic acid to form the conjugate, (e) PBA–SA and (f) PB–SA, respectively.

carboxylate and alcohol. A similar interaction also took place in xylitol–BPA (Fig. 18b). The shorter backbone, however, restricted the free rotation and limited an optimal hydrogen bonding.

Whereas the dissolution could be assisted through fructose and alditols, the role played by sialic acid has been barely reported in the literature. A study of complexation between phenyl boric acid (PBA) (Fig. 18c and d) and SA indicates that both the associated conjugates of trigonal planar boric ester (Fig. 18e) and tetrahedral borate (Fig. 18f) were obtained at pH from 2 to 9.²⁴ In our work, the pH of around 8.5 was used to generate alditol–BPA conjugates. Hence, the adjustment of pH using organic acids such as SA might yield similar results (Fig. 19a, II and III). Because the alanine side chain in BPA contains biphasic groups at physiological pH, an additional conjugate might be present (Fig. 19a, I).

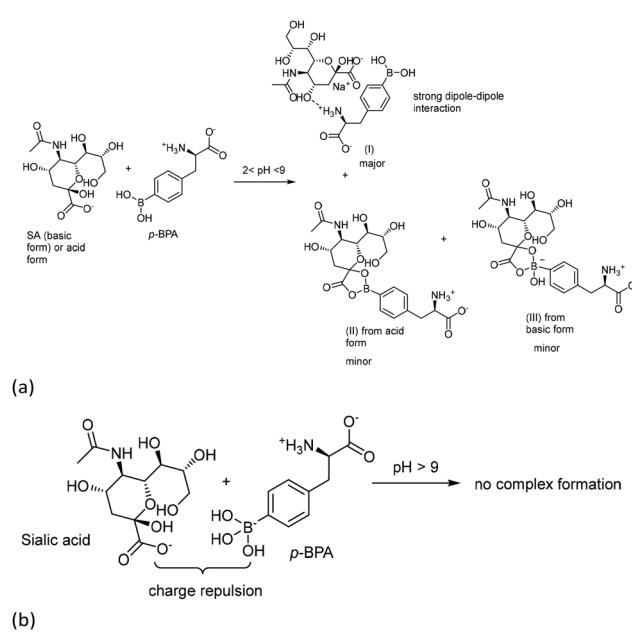


Fig. 19 (a) Energy minimization through software Chemdraw MM2 mode to derive the optimal molecular interaction between sialic acid and BPA complex (I). The conjugates (II) and (III) were hypothesized according to the literature study of phenyl boric acid and simplified phenyl borate. (b) No conjugate could be formed according to the literature.

Under alkaline conditions ($\text{pH} > 9$), the ionic tetrahedral borate could not form an SA complexing conjugate according to the reported work (Fig. 19b).²⁴ Complexes **II** and **III** were thought to be minor because either BPA–BPA or SA–BPA (**I**) conjugate exerts stronger dipole–dipole interactions. These can be evidenced from the abovementioned literature examples where only the simplified boric acid benzene was chosen as a probing model. The alanine biphasic group would complicate the study. Although alanine-containing BPA had been probed, only *meta*-BPA but not the *para* isomer was employed. *Para*-BPA induced much stronger BPA–BPA interactions. Hence, the weak interaction of *meta*-BPA–*meta*-BPA was easily disrupted by forming a hydrogen bond with H_2O . The aqueous solubility was improved by 100-fold compared with the *para*-isomer.^{12,25} Moreover, in their study, the carboxy group was intentionally protected as an ester form to minimize the undesired dipole–dipole interaction.²⁶

4. Conclusions

Alditols including sorbitol, mannitol and xylitol are complexed with BPA for improving its aqueous solubility. Among them, sorbitol–BPA exerts the highest ^1H -integral ratio. Dissolution results also show that sorbitol–BPA is the most aqueous-soluble formulation.

The samples stored at -20°C are better than those stored at room temperature in view of the long-term storage stability from HPLC analysis. These were evidenced from instantaneous dissolution and durability of the solution state as well as their physical appearance. Such a finding is also in agreement with the data from the ^1H -NMR study. Moreover, antioxidants such as $\text{Na}_2\text{S}_2\text{O}_5$ and ascorbic acid may improve the stability from both HPLC analysis and the ^1H -NMR study, whereas the differences are not statistically significant. Organic acid adjusters *i.e.* sialic acid and glutamic acid can increase the complexation ratio.

In general, all the alditol–BPA samples exert lower osmotic ratios than that of saline 0.55–0.99 *vs.* 1.0. Xylitol–BPA is the highest one with a ratio of 0.99 ± 0.11 compared with that of sorbitol–BPA, 0.83 ± 0.03 . Thus, the smaller osmotic pressure allows more dosage of BPA for loading. For example, the double-loading sorbitol–BPA combination at a concentration of 6.0% W/V provides an osmotic ratio of 1.70–1.80 lower than the expected ratio of 2, as shown in SI, Table S5. The current concentrated-acid-adjusting conditions give a lower osmotic pressure ratio of 0.8–1.0.

SEM results also showed that the complex of sorbitol–BPA produced more holes over the plastic-like microstructures. This may facilitate spontaneous water absorption during the dissolution stage.

Structural modeling using MM2 mode suggests that the longer backbone of sorbitol forms an optional hydrogen bond with BPA. Xylitol with the same stereochemical configuration but one carbon shorter forms improper hydrogen bonding. The improved dissolution of sorbitol–BPA supports the mechanistic suggestion.

In preclinical studies, the volume that can be administered to small animals, such as mice or rats, is inherently limited due to their body size and physiological tolerance. This often poses a challenge when delivering poorly soluble compounds like BPA, as large volumes may not be feasible or may compromise animal health. By improving the BPA solubility, higher doses can be delivered within the permissible volume limits, enabling more accurate dosing, minimizing variability, and enhancing the feasibility of preclinical BNCT studies.

Clinically, higher solubility improves the delivery of the required BPA dose in a smaller infusion volume and over a shorter time period. This not only reduces the treatment burden on patients, but also has the potential to benefit those with fluid-restricted conditions, such as individuals with cardiac or renal impairments, where minimizing the infusion volume is critical.

Author contributions

T.-S. Hsieh and C.-S. Yu conceived and planned the experiments. T.-S. Hsieh and C.-S. Yu carried out the experiments. J.-P. Deng and Z.-F. Yu contributed to sample preparation. Y.-H. Yu and R.-J. Sheu contributed to the interpretation of the results. C.-S. Yu took the lead in writing the manuscript. All authors provided critical feedback and helped shape the research, analysis and manuscript.

Conflicts of interest

There are no conflicts to declare.

Data availability

The authors confirm that the data supporting the finding of this study are available within the article.

Supplementary information (SI) is available. Experimental flowchart and conditions and the data of both ^1H -NMR spectra and HPLC chromatograms are provided. See DOI: <https://doi.org/10.1039/d5pm00180c>.

Acknowledgements

This research was funded by Herong Neutron Medical Corporation, Hsinchu 30261, Taiwan and the National Science and Technology of Taiwan, NSC-112-2113-M-007-014. Technical assistance was acknowledged including Mr. Kun-Yen Nie from Industrial Technology Research Institute, Ms. Huei-Chi Tan for ^1H -NMR measurement at the Department of Chemistry and Mr. Wen-Fung Liau for ICP-MS measurement at the Department of Biomedical Engineering and Environmental Sciences, Instrumentation Center at National Tsing Hua University.



References

- 1 M. Suzuki, Boron neutron capture therapy (BNCT): a unique role in radiotherapy with a view to entering the accelerator-based BNCT era, *Int. J. Clin. Oncol.*, 2020, **25**(1), 43–50.
- 2 R. F. Barth, P. Mi and W. L. Yang, Boron delivery agents for neutron capture therapy of cancer, *Cancer Commun.*, 2018, **38**, 35.
- 3 Y. Kiyanagi, Y. Sakurai, H. Kumada, H. Tanaka and P. Amer Inst, In *Status of Accelerator-Based BNCT Projects Worldwide*, 25th International Conference on the Application of Accelerators in Research and Industry (CAARI), Grapevine, TX, Aug 12–17, Grapevine, TX, 2018.
- 4 A. M. Hughes, Importance of radiobiological studies for the advancement of boron neutron capture therapy (BNCT), *Expert Rev. Mol. Med.*, 2022, **24**, e14.
- 5 T. D. Malouff, D. S. Seneviratne, D. K. Ebner, W. C. Stross, M. R. Waddle, D. M. Trifiletti and S. Krishnan, Boron Neutron Capture Therapy: A Review of Clinical Applications, *Front. Oncol.*, 2021, **11**, 601820.
- 6 R. L. Moss, Critical review, with an optimistic outlook, on Boron Neutron Capture Therapy (BNCT), *Appl. Radiat. Isot.*, 2014, **88**, 2–11.
- 7 F. Ali, N. S. Hosmane and Y. H. Zhu, Boron Chemistry for Medical Applications, *Molecules*, 2020, **25**(4), 828.
- 8 H. Xu, J. Liu, R. X. Li, J. J. Lin, L. J. Gui, Y. X. Wang, Z. Y. Jin, W. Xia, Y. H. Liu, S. J. Cheng and Z. W. Yuan, Novel promising boron agents for boron neutron capture therapy: Current status and outlook on the future, *Coord. Chem. Rev.*, 2024, **511**, 215795.
- 9 X. M. Li, P. Y. He, Y. J. Wei, C. H. Qu, F. T. Tang and Y. M. Li, Application and perspectives of nanomaterials in boron neutron capture therapy of tumors, *Cancer Nanotechnol.*, 2025, **16**, 25.
- 10 S. W. Xu, Y. Yu, B. Y. Zhang, K. J. Zhu, Y. Cheng and T. Zhang, Boron carbide nanoparticles for boron neutron capture therapy, *RSC Adv.*, 2025, **15**(14), 10717–10730.
- 11 X. P. Chen, F. C. Hsu, K. Y. Huang, T. S. Hsieh, S. S. Farn, R. J. Sheu and C. S. Yu, Fluorine-18 labeling PEGylated 6-boronotryptophan for PET scanning of mice for assessing the pharmacokinetics for boron neutron capture therapy of brain tumors, *Bioorg. Med. Chem. Lett.*, 2024, **105**, 129744.
- 12 J. P. Deng and C. S. Yu, Recent Development of Radiofluorination of Boron Agents for Boron Neutron Capture Therapy of Tumor: Creation of 18F-Labeled C-F and B-F Linkages, *Pharmaceuticals*, 2023, **16**, 93.
- 13 Y. Q. Zhou, Z. L. Peng, E. S. Seven and R. M. Leblanc, Crossing the blood-brain barrier with nanoparticles, *J. Controlled Release*, 2018, **270**, 290–303.
- 14 Y. Kanai, Amino acid transporter LAT1 (SLC7A5) as a molecular target for cancer diagnosis and therapeutics, *Pharmacol. Ther.*, 2022, **230**, 107964.
- 15 H. Nakashima, The New Generation of Particle Therapy Focused on Boron Element (Boron Neutron Capture Therapy; BNCT) - The World's First Approved BNCT Drug, *Yakugaku Zasshi*, 2022, **142**(2), 155–164.
- 16 R. F. Barth, N. Gupta and S. Kawabata, Evaluation of sodium borocaptate (BSH) and boronophenylalanine (BPA) as boron delivery agents for neutron capture therapy (NCT) of cancer: an update and a guide for the future clinical evaluation of new boron delivery agents for NCT, *Cancer Commun.*, 2024, **44**(8), 893–909.
- 17 M. I. Yasawy, U. R. Folsch, W. E. Schmidt and M. Schwend, Adult hereditary fructose intolerance, *World J. Gastroenterol.*, 2009, **15**(19), 2412–2413.
- 18 G. Halbert, M. Elliott, S. Ford, L. Dick and E. Schmidt, Improved pharmaceutical stability of a boronphenylalanine mannitol formulation for boron neutron capture therapy, *Eur. J. Pharm. Sci.*, 2013, **48**(4–5), 735–739.
- 19 S. Heikkinen, S. Savolainen and P. Melkko, In Vitro Studies on Stability of L-p-boronophenylalanine-fructose Complex (BPA-F), *J. Radiat. Res.*, 2011, **52**(3), 360–364.
- 20 P. Bendel, C. Anderson and G. W. Kabalka, in *Structure of the BPA-Fructose Complex. In Frontiers in Neutron Capture Therapy*, ed. M. F. Hawthorne, K. Shelly and R. J. Wiersema, Springer US, Boston, MA, 2001, vol. 1, pp. 869–874.
- 21 T. Watanabe, T. Yoshikawa, H. Tanaka, Y. Kinashi, G. Kashino, S. Masunaga, T. Hayashi, K. Uehara, K. Ono and M. Suzuki, Pharmacokinetic Study of 14C-Radiolabeled p-Boronophenylalanine (BPA) in Sorbitol Solution and the Treatment Outcome of BPA-Based Boron Neutron Capture Therapy on a Tumor-Bearing Mouse Model, *Eur. J. Drug Metab. Pharmacokinet.*, 2023, **48**(4), 443–453.
- 22 Y. Hattori, T. Andoh, S. Kawabata, N. N. R. Hu, H. Michiue, H. Nakamura, T. Nomoto, M. Suzuki, T. Takata, H. Tanaka, T. Watanabe and K. Ono, Proposal of recommended experimental protocols for in vitro and in vivo evaluation methods of boron agents for neutron capture therapy, *J. Radiat. Res.*, 2023, **64**(6), 859–869.
- 23 Z. Luo, W. Huang, F. Li, Z. Tang, S. Han, X. Zhang and Z. Zhao, *Freeze-drying process applied to L-BPA*, CN103100094, 2013.
- 24 K. Djanashvili, L. Frullano and J. A. Peters, Molecular recognition of sialic acid end groups by phenylboronates, *Chem. – Eur. J.*, 2005, **11**(13), 4010–4018.
- 25 N. Kondo, F. Hirano and T. Temma, Evaluation of 3-Borono-1-Phenylalanine as a Water-Soluble Boron Neutron Capture Therapy Agent, *Pharmaceutics*, 2022, **14**(5), 1106.
- 26 H. Otsuka, E. Uchimura, H. Koshino, T. Okano and K. Kataoka, Anomalous binding profile of phenylboronic acid with N-acetylneurameric acid (Neu5Ac) in aqueous solution with varying pH, *J. Am. Chem. Soc.*, 2003, **125**(12), 3493–3502.

